REPORT DOCUMENTATION PAGE

Form Approved
OMB NO. 0704-0188

1. AGENCY USE ONLY (Leave Blank)	2. REPORT DATE	3. REPORT TYPE AND DATES COVERED

4. TITLE AND SUBTITLE

Risk Mitigation for HTS Motors: Intermediate Temperature (27 K) Strain Effects in Reinforced Bi-Sr-Ca-Cu-O Superconductors

5. FUNDING NUMBERS

6. AUTHOR(S)

Justin Schwartz

7. PERFORMING ORGANIZATION NAME(S) AND ADDRESS(ES)

Florida State University

8. PERFORMING ORGANIZATION REPORT NUMBER

9. SPONSORING / MONITORING AGENCY NAME(S) AND ADDRESS(ES)

U. S. Army Research Office
P.O. Box 12211
Research Triangle Park, NC 27709-2211

10. SPONSORING / MONITORING AGENCY REPORT NUMBER

11. SUPPLEMENTARY NOTES

The views, opinions and/or findings contained in this report are those of the author(s) and should not be construed as an official Department of the Army position, policy or decision, unless so designated by other documentation.

12 a. DISTRIBUTION / AVAILABILITY STATEMENT

Approved for public release; distribution unlimited.

12 b. DISTRIBUTION CODE

13. ABSTRACT (Maximum 200 words)

High temperature superconductors , known for their high critical temperatures, also have very high upper critical fields and thus have received significant attention for superconducting magnets (SCMs). To operate in a SCM, however, the superconductor must have high Jc in the presence of high magnetic field and under the action of mechanical strain (•) that results from the manufacturing processes, differential thermal contraction, and Lorentz forces. For some HTS applications, the effects of mechanical strain on Jc limit the system performance and lifetime, thus posing the most serious risk to successful lifetime operation. Past results at FSU indicated that the effects of longitudinal compression (in the current carrying "abr" direction) on Jc are critical. These experiments, which studied the effects of longitudinal compression applied at room temperature and at 77 K, clearly showed that the effects of strain became more serious as the temperature decreased. Since many applications are expected to operate around 30 K, minimizing risk necessitates understanding the effects of abr compressive strains at lower temperature. The NHMFL has recently developed a large bore dewar specifically designed to house a neon liquifier that feeds liquid directly to a large bath-cooled sample space. The sample space is sufficient in size and flexibility to accommodate tensile and compressive experiments on short sample conductors and to perform Lorentz-force tests on coils.
Here we report on the progress towards measuring the effects of stress and strain on the transport Jc of BSCCO and YBCO. We report progress on measurements at room temperature and on the development of a fatigue-stress-strain-Jc probe that will operate in

14. SUBJECT TERMS

15. NUMBER OF PAGES

16. PRICE CODE

17. SECURITY CLASSIFICATION OR REPORT	18. SECURITY CLASSIFICATION ON THIS PAGE	19. SECURITY CLASSIFICATION OF ABSTRACT	20. LIMITATION OF ABSTRACT
UNCLASSIFIED	**UNCLASSIFIED**	**UNCLASSIFIED**	**UL**

NSN 7540-01-280-5500

Standard Form 298 (Rev.2-89)
Prescribed by ANSI Std. 239-18
298-102

Enclosure 1

BEST AVAILABLE COPY

FINAL REPORT

Risk Mitigation for HTS Motors Intermediate Temperature (27 K) Strain Effects in Reinforced Bi-Sr-Ca-Cu-O Superconductors

Submitted to the Office of Naval Research

Justin Schwartz
Florida State University

June 7, 2004

Introduction

High temperature superconductors (HTS), known for their high critical temperatures, also have very high upper critical fields and thus have received significant attention for superconducting magnets (SCMs). To operate in a SCM, however, the superconductor must have high J_c in the presence of high magnetic field and under the action of mechanical strain (ε) that results from the manufacturing processes, differential thermal contraction, and Lorentz forces. For some HTS applications, the effects of mechanical strain on J_c limit the system performance and lifetime, thus posing the most serious risk to successful lifetime operation. Past results at FSU indicated that the effects of longitudinal compression (in the current carrying "abr" direction) on J_c are critical. These experiments, which studied the effects of longitudinal compression applied at room temperature and at 77 K, clearly showed that the effects of strain became more serious as the temperature decreased. Since many applications are expected to operate around 30 K, minimizing risk necessitates understanding the effects of abr compressive strains at lower temperature. The NHMFL has recently developed a large bore dewar specifically designed to house a neon liquifier that feeds liquid directly to a large bath-cooled sample space. The sample space is sufficient in size and flexibility to accommodate tensile and compressive experiments on short sample conductors and to perform Lorentz-force tests on coils.

Here we report on the progress towards measuring the effects of stress and strain on the transport J_c of BSCCO and YBCO. We report progress on measurements at room temperature and on the development of a fatigue-stress-strain-I_c probe that will operate in conjunction with the liquid neon condenser to facilitate the 27 K measurements.

Results

YBCO coated conductor

Samples

YBCO coated conductor samples were supplied by American Superconductor Corporation and had the following architecture: a substrate layer made of 75 μm thick RABiTS type Ni-5at%W was coated with a 2 μm Ni layer, a 50 nm thick Y_2O_3 seed layer, a 250 YSZ barrier layer, and a 20 nm CeO_2 cap layer. The YBCO layer was 1 μm thick, deposited using a trifluoroacetates (TFA) based solution process. The Ag cap layer was 3 μm thick. The tape cross-sectional area is 10 mm wide by 0.085 mm thick. For these experiments, samples were cut to 25-30 mm lengths. The critical current measured at 77 K, self-field, at $\epsilon = 0$ is 146.5 A.

Electro-Mechanical Testing

The room temperature linear tensile testing device [1] was used to measure the mechanical properties and to apply mechanical strain ε in determining ε-I_c behavior. A linear variable displacement transducer was used to measure displacement and a load cell was used to measure load. The displacement and load were converted to strain and stress respectively using LabVIEW software. The properties determined are Young's modulus; yield stress, and ultimate strength. Individual samples were subjected to a single value of uniaxial tensile strain for determining ε-I_c performance. Thus the performance variations are associated with small sample-to-sample

variations. The strain ranged from 0.00% to ~ 1.0%. I_c was measured at 77 K, self-field, using the four-point method and a 1μV/cm criterion.

Microstructural Analysis

The microstructure of each sample was analyzed after straining and electrical testing to evaluate the mechanism of mechanically induced failure. The samples were etched to remove the silver cap layer and expose the YBCO. The etching solution was a mixture of ammonium hydroxide (NH_4OH), hydrogen peroxide (H_2O_2) and methanol (CH_3OH) in a 1:1:4 ratio by volume. After etching, the samples were mounted on a sample carrier and loaded in the Environmental Scanning Electron Microscope (ESEM) for microstructural analysis.

Results

A tensile stress-strain curve is shown in Figure 1. The mechanical properties obtained from the tensile test are shown is Table 1. ε-I_c results are presented in Figure 2 and the corresponding *n*-value-strain results are presented in Figure 3. The ε-I_c results show no degradation of critical current up to $\varepsilon \sim 0.75\%$. At $\varepsilon = 0.8\%$, the current degraded sharply to <50% of the unstrained sample. The critical current degraded further to 25% of unstrained sample at $\varepsilon = 1\%$.

These results are different from those results reported by Thieme *et al.* [2] and van der Laan [3] in which degradation was seen at $\varepsilon \sim 0.5\%$. This difference arises since the temperature at which straining was done for the two cases are different, i.e. room temperature in this case and 76 K in the referred cases. Thus, there is significant difference in the ε-I_c results depending on the straining temperature. Further, differences in the results are also due to different experimental setups between this work and referred cases.

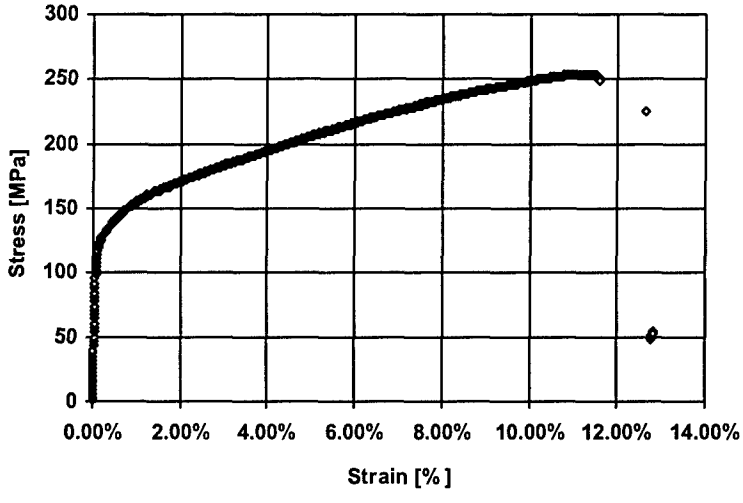

FIGURE 1. Room temperature stress-strain curve for YBCO coated conductor. Resulting properties are listed in Table 1.

TABLE 1. Room temperature mechanical properties of coated YBCO conductor obtained from the tensile test.

Property	Value Obtained
Young's Modulus	110 GPa
Yield Stress (based on 0.2% off-set)	130 MPa
Ultimate Tensile Stress	254 MPa

Furthermore, axial straining of YBCO coated conductor at room temperature, which can be regarded as equivalent to pre-tensioning of the conductor during coil winding, does not cause degradation on the superconducting properties up to $\varepsilon \sim 0.75\%$.

The strain-*n*-value results show a two-stage reduction in *n*-value with increasing strain. The first stage from $n = 35$ at $\varepsilon = 0\%$ to $n = 26$ at $\varepsilon \sim 0.1\%$. The second stage reduction is seen from $n = 22$ at $\varepsilon \sim 0.8\%$ 0 to $n = 18.7$ at $\varepsilon \sim 1\%$. These results differ from those reported [2] in which there was a slight increase in *n* from $\varepsilon = 0\%$ to $\varepsilon \sim 0.5\%$ followed with a sharp drop in *n*-value beyond $\varepsilon \sim 0.5\%$. The first stage reduction in *n* can be due to handling of samples since the sample at $\varepsilon = 0\%$ was never mounted on the room temperature straining device, but was directly cooled to 77 K for I_c measurement. The second stage reduction in *n*-value is due to degradation of critical current as strain was increased.

ESEM micrographs are presented in Figures 4 for increasing strain. No cracks are observed for samples strained between up to 0.75%. Samples strained at 0.8% and above, however, show cracks, with the amount of cracks increasing with strain.

YBCO conclusions

A strain limit of 0.75% was observed in the ε-I_c data. The *n*-value was reduced irreversibly on the second stage at which I_c degraded sharply. The ESEM microstructural analysis do not show cracks for samples that were strained up to $\varepsilon \sim 0.75\%$ but shows cracks for samples strained beyond $\varepsilon = 0.75\%$. It is therefore clear that cracks observed in the YBCO coated conductor samples that were strained beyond $\varepsilon = 0.75\%$ are the cause of I_c degradation. Furthermore, operations that induce fatigue in the conductor may require a lower strain limit. Results for fatigue experiments will be forthcoming.

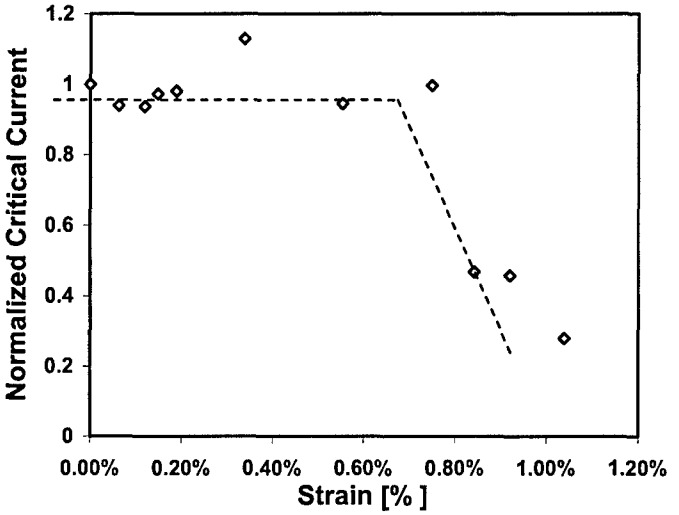

FIGURE 2. Tensile ε-I_c results for YBCO coated conductor. Dashed lines are placed as guides to the eye.

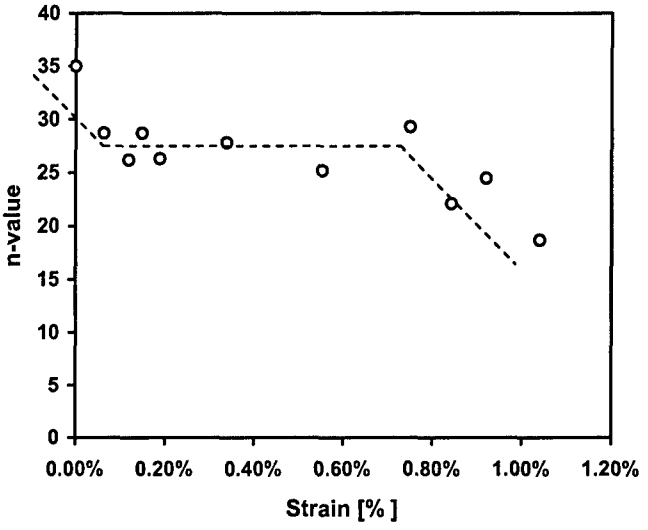

FIGURE 3. Results for *n*-value-strain for YBCO conductor. Dashed lines are shown as guide to the eye.

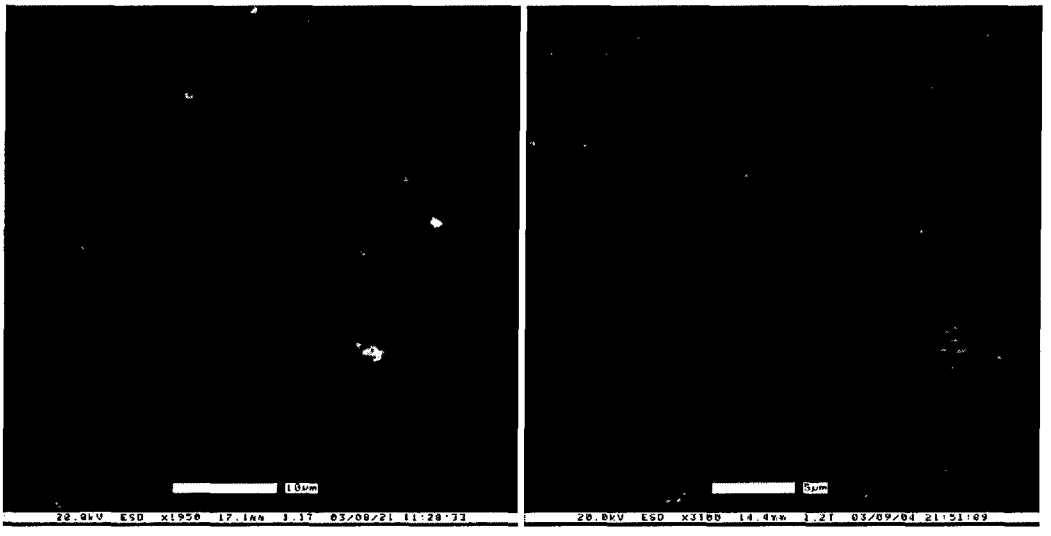

(a) ε =0%

(b) ε = 0.7%

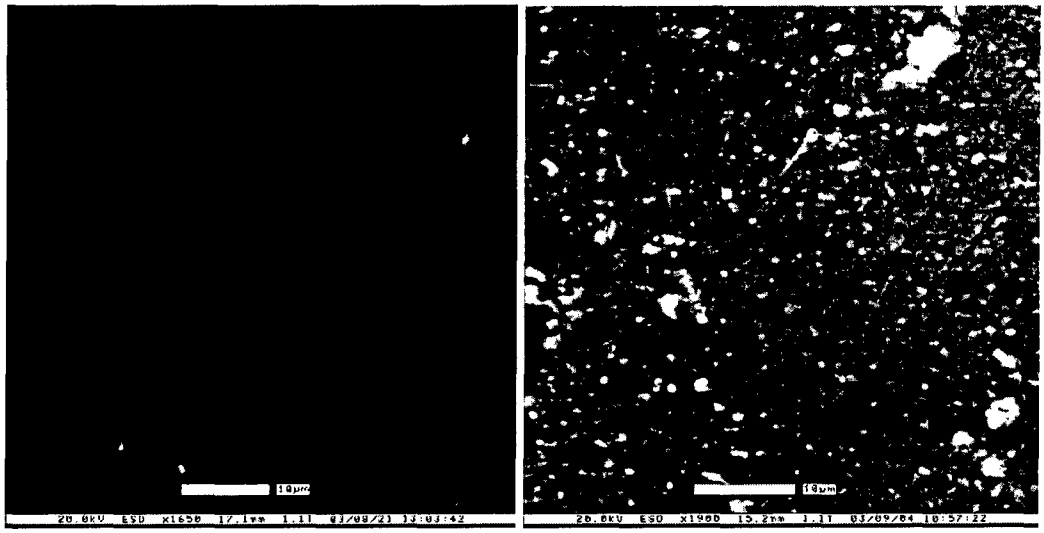

(c) $\varepsilon = 0.8\%$ (d) $\varepsilon = 1.0\%$

FIGURE 4. ESEM micrographs of YBCO coated conductor after applying different level of strains.

BSCCO conductors

Samples

Here we report on measurements using samples from one batch of AgMg sheathed Bi-2212 multifilamentry tape that was supplied by Oxford Superconducting Technologies Inc. (OST). During manufacturing, a visual inspection was done on the tape and sections that had bubbles after the intermediate heat treatment were marked and the fabrication process completed. The bubbled sections were separated from the bubble-free ones after the final reaction. From these two categories *i.e.* bubbled and bubble-free categories, a number of 45-mm long samples were prepared and used for tensile tests and strain-I_c measurements.

Tensile Tests

Samples from the bubbled and bubble-free sections were subjected to uniaxial tensile tests on the linear tensile testing device. The aim of this was to determine whether the two sections would have different mechanical properties. Each sample was tested at room temperature until breaking occurred. For each category, samples were tested according to the following conditions:

i) Full elongation to failure without a reload cycle.
ii) Elongation to failure with a reload at 0.15% strain.
iii) Elongation to failure with a reload at 0.50% strain.
iv) Elongation to failure with reload at 0.70% strain.

I_c-Strain Tests

Other samples from the two categories were used to determine the influence of bubbles on critical current, I_c. A total of 36 samples were used for each category and three samples for a set value of strain. Samples were uniaxially strained to a particular strain value and subsequently I_c was measured. Each sample was only used once, and the strain level was increased from one sample to another to cover a range from 0.1% to ~ 0.5%. I_c measurements were carried at 4.2 K self-field, using a four-point method with 1μV/cm criterion.

Microstructural Analysis

Some samples from the two categories were prepared for microstructural analysis. The samples were cut along the longitudinal direction and cold moulded with epoxy. The samples were then polished and viewed on an optical microscope; images were captured by SigmaScan Pro.

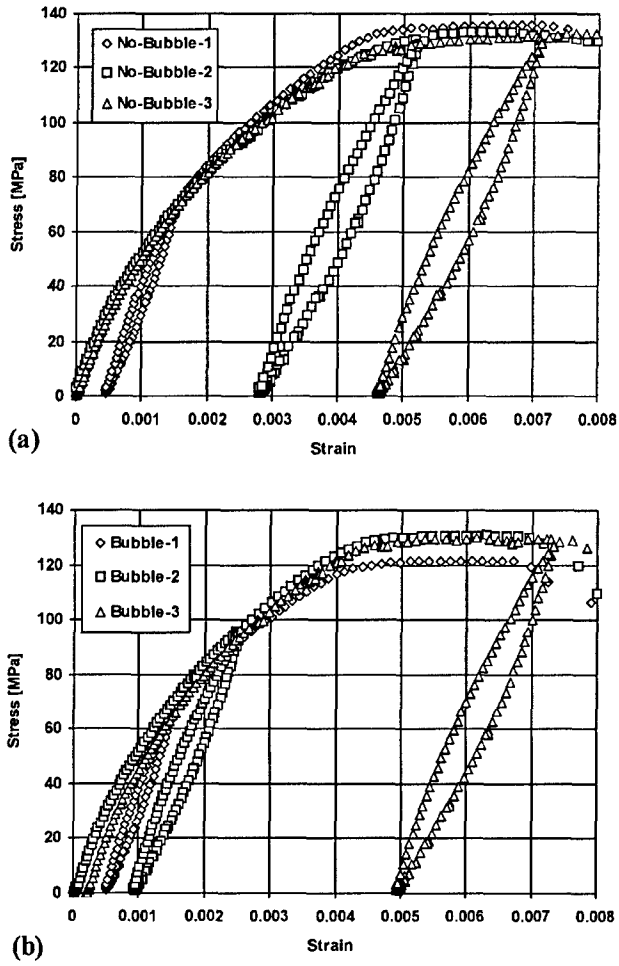

Figure 5. σ–ε for (a) bubble-free and (b) bubbled sections of the AgMg sheathed Bi-2212 tape.

Results

Figures 5 (a) and (b) are the results for tensile tests for bubble-free and bubbled samples, respectively. They show that some sections with bubbles have low ultimate strength (120 MPa) while some have their ultimate strength comparable to bubble-free sections (130 MPa). However in applications we do not subject tapes to such high stress because the strain levels at this stress approach the marginal level required to cause I_c degradation.

The Young's Modulus E, calculated from the return lines ranges from 52 to 64 GPa for bubbled sections and from 51 to 63 GPa for bubble-free sections at 0.15% and 0.70% return strain levels, respectively. These values are close for a given strain value for both sections indicating that the bubbles do not cause any significant change on the mechanical properties at the useful range of stresses for the tape.

The strain-I_c results are presented in Figure 6. The bubbled sections had lower I_c in most of the data compared to bubble-free sections, including the zero-strain I_c values. The average I_c values at zero-strain are 488.5 A and 369.4 A for bubble-free and bubbled sections, respectively. Continuous and dashed lines are trend lines for bubble-free and bubbled sections, respectively.

Figures 7 and 8 show σ–ε–I_c relationships for bubble-free and bubbled sections, respectively. The solid lines represent the I_c-ε trend while the dashed line represents the σ–ε curves. Note that there is a scatter of data for both I_c and stress in both cases since each point represents a new sample.

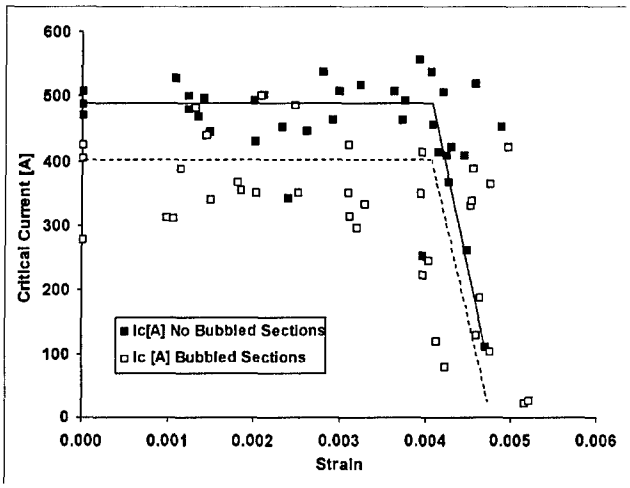

Figure 6. I_c-ε results for bubble and bubbled-free sections of AgMg sheathed Bi-2212 tape. Solid square marks are for bubble-free sections and hollow squares marks are for bubbled sections of the tape. Each mark represents a new sample.

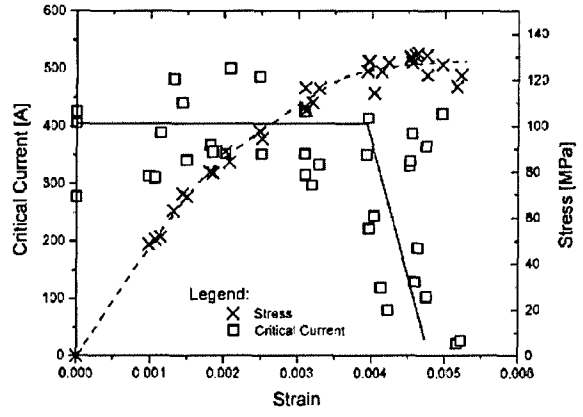

Figure 7. σ–ε-I_c results for bubble free sections of the AgMg sheathed Bi-2212 tape.

Figures 9 (a) and (b) show the different micrographs for bubble-free sections while Figures 10 (a) and (b) are for bubbled sections. Note that filament irregularities exist in bubble-free sections (Figures 9 (a) and (b)). Voids are seen in the superconducting filament areas in Figures 10 (a) and (b) and are related to the size and numbers of bubbles originally present in the section before they were removed by the rolling process. Consequently the size and the number of voids vary from one section to another as seen in Fig 10 (a) and (b).

The σ–ε results showed that some sections of the bubbled area of the tape have lower strength than other sections while the bubble-free sections have the same ultimate strength. This is explained by the fact that we do not know the differences amongst the bubbled sections in terms of bubble sizes and their number. It is likely that the sections with the same ultimate strength as the bubble-free section may have small size bubbles that were not detected.

The results for I_c-ε show that the bubbled sections carry less superconducting current than bubble-free sections, but the normalized I_c have similar trends. This is explained by the fact that the filaments in bubble-free sections do not contain voids while the bubbled section contain voids as shown in figures 5 and 6. It is clear that presence of bubbles at the intermediate manufacturing stage impedes the current carrying capacity of the fully processed conductor. The number and size of bubbles in a particular section determines the superconducting properties of the section, and thus for a long tape, the bubbled sections will limit the superconducting properties.

BSCCO conclusions

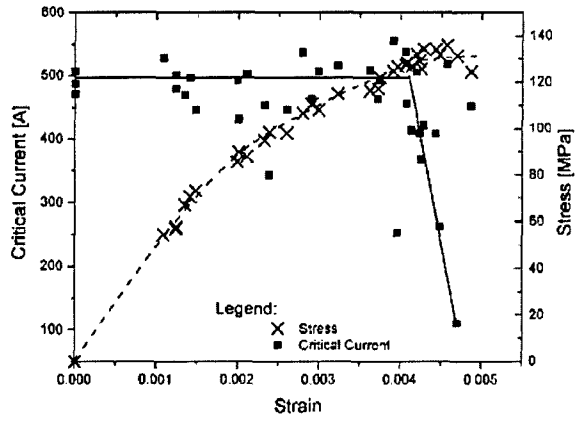

Figure 8. σ–$\tilde{\varepsilon}$-I_c results for bubbles sections of the AgMg sheathed Bi-2212 tape.

The presence of bubbles does not cause significant changes in the mechanical properties at the useful range of stresses for the tape, but impede its current carrying capacity. The number and size of bubbles in a particular section determines the superconducting properties. Thus, for a long superconducting tape, the bubbled sections limit the superconducting properties. Minimizing bubble formation during the manufacturing process is important for enhancing properties for Bi-2212 tapes. This can be done by using powders with less than 200-ppm carbon content [4] and by controlling other parameters that enhance the formation of bubbles such as atmosphere, the heating rate and melting temperature.

27 K stress-strain probed development

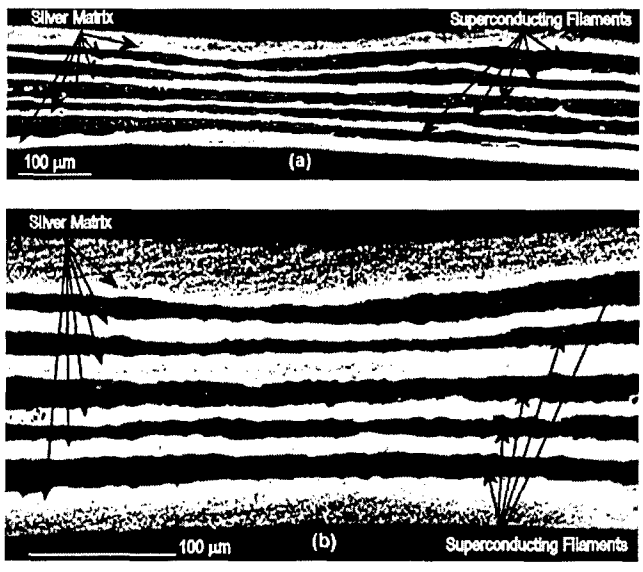

Figure 9 (a) and (b). Optical microscopy images for longitudinal cross-sections of the bubble-free parts of the AgMg sheathed Bi-2212 tape. The bright areas are the Ag Matrix and the dark areas are the Bi-2212 filaments.

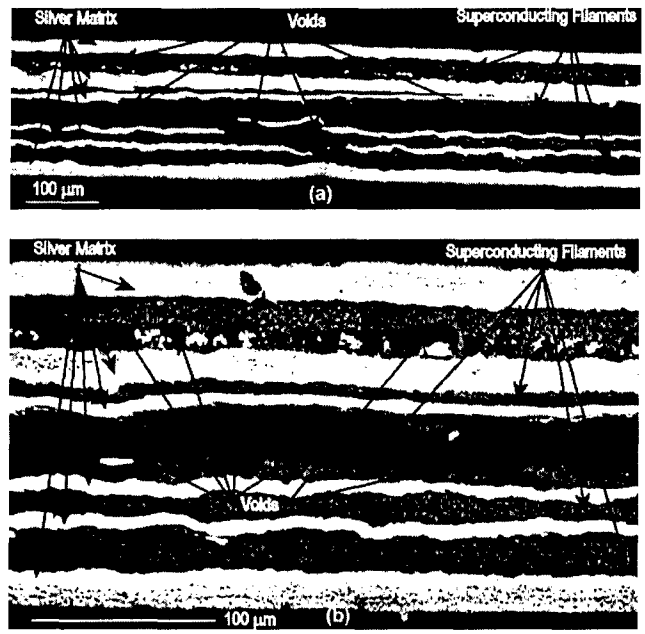

Figure 10 (a) and (b). Optical microscopy images for a longitudinal cross section of the bubbled parts of the tape. The bright areas are the Ag Matrix and the dark areas are the Bi-2212 filaments. Black areas in the filaments are voids.

Currently a new probe design, allowing parallel mechanical and electrical in-field characterization of short superconducting samples is under construction and will soon be available for experiments. Since it is planned to measure a number of samples without warming up the entire system, a probe with reduced thermal capacity and a load–lock through which the sample enters the Ne-bath has been conceived. This requires running the liquefier in a satellite

dewar. The load-lock will also help to avoid condensation and freezing of air on the moving parts of the experiment. Up to 5 *cm* short samples can be mounted between two calipers on a mechanical testing device at the bottom of the probe, which is operated over a worm gear by a stepper motor (Parker Automation, Inc.) outside of the cryostat. The device is rated for loads up to 1 *kN*. Schematic views are presented in Figures 11 and 12. The calipers are electrically insulated against the rest of the device and can be connected to the coaxial current lead to pass a transport current through the sample. The sample elongation is measured *in-situ* by a precision optical displacement sensor supplied by Philtec Inc. with a resolution of about 0.1 μm. The applied load is measured *in-situ* by a low-temperature resistive load-cell supplied by A.L. Design, Inc.

FIGURE 11. Cross sectional view of the new probe design plus load lock.

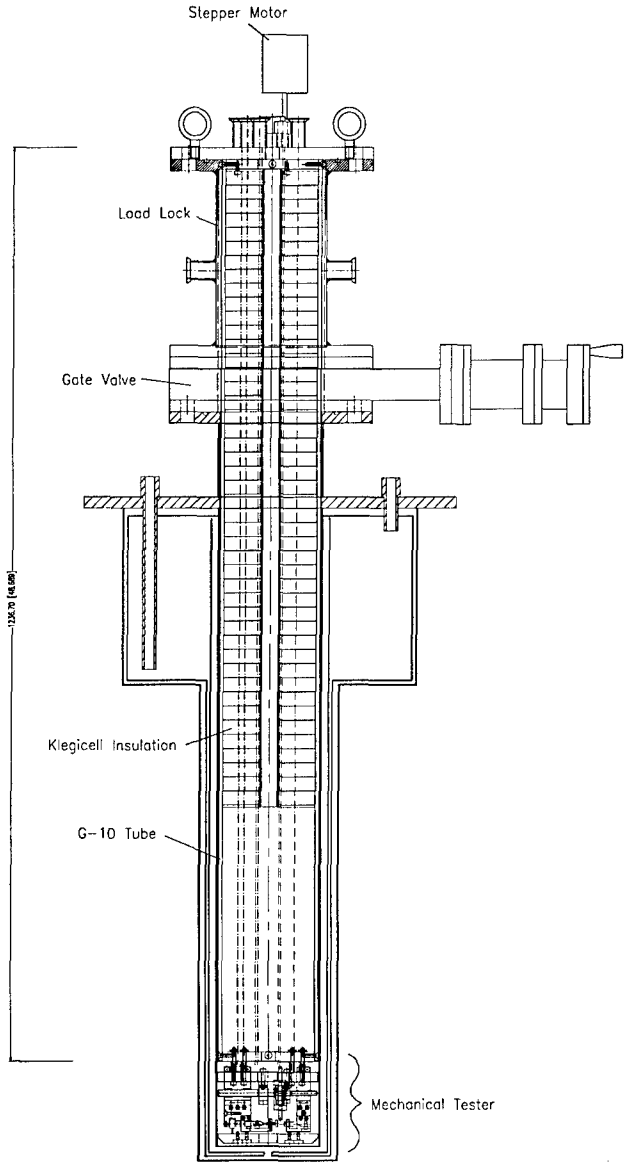

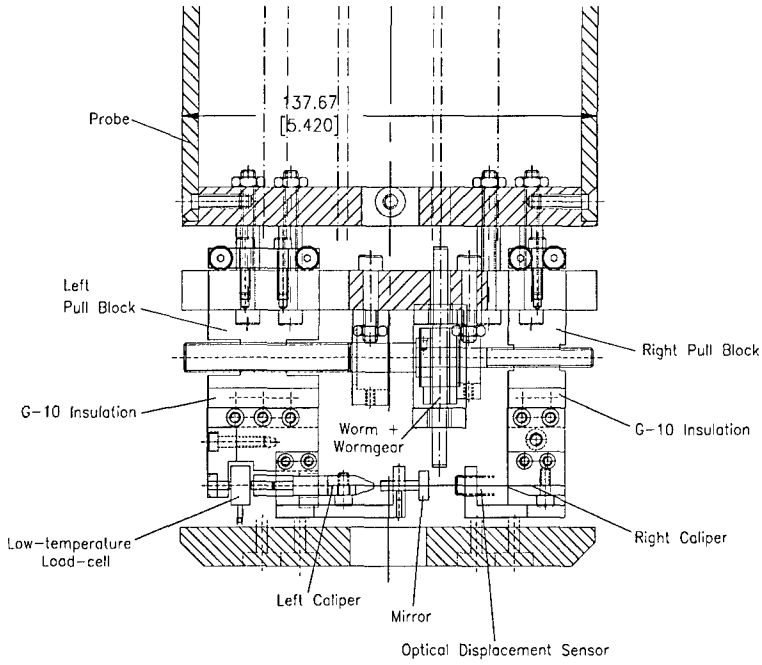

FIGURE 12. Detail view of the low temperature mechanical/electrical testing device (bottom part in Figure 11).

References

[1] J. Schwartz, B. C. Amm, H. Garmestani, D. K. Hilton and Y. Hascicek, "Mechanical Properties and Strain Effects in $Bi_2Sr_2CaCu_2O_x$/AgMg Composite Conductors", *IEEE Trans.App. Supercond*, Vol. 7, pp. 2038-2041, 1997.

[2] C.L.H. Thieme, E. Fleshler, D.M. Buczek, M. Jowett, L.G. Fritzemeier, P.N. Arendt, S.R. Foltyn, J.Y. Coulter and J.O. Willis, "Axial Strain Dependence at 77K of the Critical Current of Thick YbaCuO Films on Ni-Alloy Substrates with IBAD Buffer Layers," in *IEEE Transactions on Applied Superconductivity,* Vol. 9, 1999, pp. 1494 –1497.

[3] D.C. van de Laan, H. J. N. van Eck, B. ten Haken, H. H. J. ten Kate and J. Schwartz, "Strain Effects in High Temperature Superconductors Investigated With Magneto-Optical Imaging," in *IEEE Transactions on Applied Superconductivity,* Vol. 13, 2003, pp. 3534-3539.

[4] H. Miao, K. R. Marken, J. Sowa, J. A. Parrell, and S. Hong. "Long length AgMg clad Bi-2212 multifilamentary tapes," *Adv. in Cryogenic Engineering*, Vol. 48, pp. 709-716, 2002.

Publications resulting from this support

1. U.P. Trociewitz, H.J.N van Eck, S.H. Thompson, A. Mbaruku, H. Weijers, and J. Schwartz, "Development of a LNe Test Facility," Advances in Cryogenic Engineering 47A, Cryogenic Engineering Conference, 139-146 (2002)
2. D.C. van der Laan, M.W. Davidson, B. ten Haken, H.H.J. ten Kate, and J. Schwartz, "Magneto-Optical Imaging study of the crack formation in superconducting tapes caused by applied strain," *Physica C* **372-376** 1020-1023 (2002)
3. A. L. Mbaruku, K. R. Marken, M. Meinesz, H. Miao, P. V. P. S. S. Sastry, and J. Schwartz, "Effect of Processing Defects on Stress-Strain-I_c for AgMg Sheathed Bi-2212 tapes," *IEEE Transactions on Applied Superconductivity* **13**(2) 3522-3525 (2003)
4. A.L. Mbaruku, I. Rutel, U.P. Trociewitz, H.W. Weijers, and J. Schwartz, "Electro-Mechanical Behavior of YBCO Coated Conductor in Tension," International Cryogenic Materials Conference, Anchorage, Alaska (accepted 2003)